

## Power Consumption in Mixing and Aerating of Shear Thinning Fluid in a Stirred Vessel

A. Bombač\*, M. Žumer\*\*, and I. Žun

University of Ljubljana, Faculty of Mechanical Engineering, LFDT,  
Aškerčeva 6, 1000 Ljubljana, Slovenia

\*\* University of Ljubljana, Faculty of Chemistry and Chemical Engineering,  
Aškerčeva 5, 1000 Ljubljana, Slovenia

Original scientific paper

Received: April 22, 2006

Accepted: September 16, 2006

The paper presents an analysis of power consumption in mixing and dispersing of air into a shear thinning fluid in a standard cylindrical vessel stirred with a Rushton turbine. Water-CMC solutions at  $w = 0.5\%$  and  $w = 1\%$  mass fraction and compressed air were used. The apparent viscosity enabling the power vs. Reynolds number relation was calculated using the Metzner-Otto method. A comparison of the power-consumption measurement results in single-phase mixing is in good agreement with the results found in the literature.

When air is dispersed into a shear thinning fluid, an obvious reduction of power consumption can be noticed especially at higher impeller speeds and gas flow rates, which is more noticeable in an  $w = 0.5\%$  than in an  $1.0\%$  CMC solution. In fact, the dissipated mixing power depended on gas-filled cavity structures behind the blades, which affected the impeller pumping efficiency. All experimental flow regimes were analyzed and depicted in a generalized flow regime map as Froude vs. Flow number dependence. Developing of structures was shown from high effective to low effective operation, e.g. complete dispersion and bubble column operation, respectively. Mixing power was found to be independent of airflow rate at low Reynolds numbers. A comparison of the measured values in air-dispersion and the results from correlations found in the literature confirms a general trend of impeller power reduction.

*Key words:*

Mixing, aerating, power consumption, cavity structures, rheology, carboxymethyl cellulose, Rushton turbine

### Introduction

In many technological processes, e.g. broth fermentation in the pharmaceuticals industry air-dispersion into rheologically complex fluids has been performed by turbine impellers. Due to the changed rheological properties of the broth during the process, the mixing intensity can be changed with respect to the initial state. A question arises of how the change in viscosity influences the mixing power in stirring the liquid and in the dispersing of gases into such fluid with a turbine impeller. Transformation from a Newtonian (low viscosity fluid at the beginning of fermentation) to a non-Newtonian fluid (high viscosity at the end of the process) can cause a change in viscosity at a magnitude rate of 100 or more. The viscosity then becomes the most important parameter, which then dictates the hydrodynamics of the liquid bulk. To avoid complexities within the biological process where most of the properties change over time, the fluids used for research studies, such as glycerol, carboxymethyl cel-

lulose (CMC) and xanthan gum, are often used as model fluids. The latter two were found to be suitable for the study of the quality of agitation, systematic investigation of flows generated by a disk turbine,<sup>11</sup> to reveal the effect of pseudoplasticity on gas hold-up,<sup>16</sup> gas-filled cavity structures,<sup>3</sup> power requirements in a mixing vessel,<sup>6,8–10,13,14</sup> flooding transition,<sup>6</sup> or to test CFD-study results,<sup>12</sup> etc.

This study, carried out with a non-Newtonian CMC fluid, aims to contribute to previous studies on the analysis of power consumption in mixing and aerating in a standard cylindrical vessel stirred with a Rushton turbine.

### Experimental

#### Equipment

Dispersion of air into a water solution of CMC was done in a cylindrical vessel of  $T = 450$  mm equipped with four baffles of width  $T/10$  with a flat bottom and rounded edges. A standard Rushton turbine of 150 mm diameter at clearance  $T/3$  was used

\* Corresponding author: andrej.bombac@fs.uni-lj.si

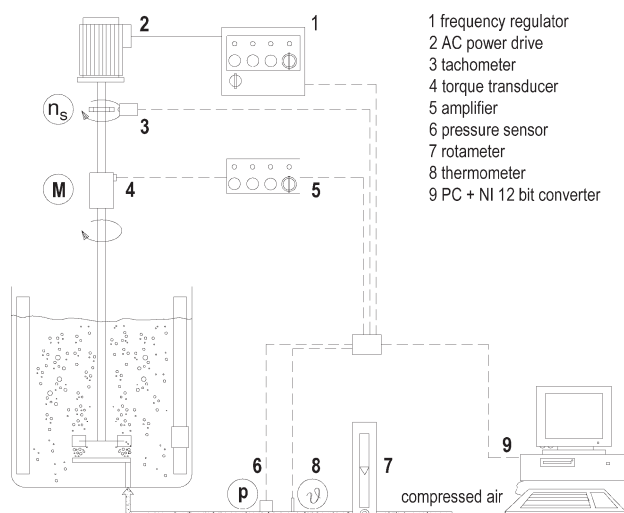


Fig. 1 – Experimental setup

in all experiments. The geometrical configuration and setup are schematically depicted in Fig. 1, and described in detail elsewhere.<sup>1–4,17</sup> Impeller rotational speed and gas flow rate were varied through two sets of measurements, as follows: (set #1) at three constant gas flow rates i. e.  $Q = 1.55, 2.5$  and  $5 \text{ m}^3 \text{ h}^{-1}$ , the rotational speed (kept constant while measuring) was increased stepwise from  $n_s = 50$  to  $614 \text{ min}^{-1}$ , and (set #2) at four constant rotational speeds, i. e.  $n_s = 153, 266, 376$  and  $460 \text{ min}^{-1}$ , where the gas flow rate (kept constant while measuring) was increased stepwise from  $Q = 0.37$  to  $3.62 \text{ m}^3 \text{ h}^{-1}$ , respectively.

The non-Newtonian fluids used as model fluids were aqueous solutions of Carboxymethyl Cellulose (manufacturer Aqualon) at two mass fraction:  $w = 0.5$  and  $1 \%$ , respectively. Compressed air was used for air-dispersion in CMC fluids. In all experiments, the fluid temperatures were measured and varied between  $20$  and  $23 \text{ }^\circ\text{C}$ .

### Shear thinning fluid

Knowledge of the transport properties of the fluid used in the experiment is of fundamental importance to describe the phenomenon with dimensionless numbers and particularly in the case when the property is strongly dependent on temperature. For this reason, the properties of water and CMC solutions were measured at  $20 \text{ }^\circ\text{C}$  and are presented in Table 1.

One distinctive feature of shear thinning fluids is that they do not exhibit certain finite shear stresses.  $\tau$  do not change linearly with increasing shear rate  $\dot{\gamma}$ , while the apparent viscosity  $\eta_a$  decreases with increasing  $\dot{\gamma}$ . At very high or at very low  $\dot{\gamma}$ , the relation of  $\tau$  vs.  $\dot{\gamma}$  is almost linear, other-

Table 1 – Transport properties of aqueous CMC solutions and water at  $\vartheta = 20 \text{ }^\circ\text{C}$ 

Fluid	$\sigma/\text{N m}^{-1}$	$\rho/\text{kg m}^{-3}$
$w = 0.5 \%$ CMC	0.071	1000
$w = 1.0 \%$ CMC	0.070	1002
water	0.075	998

wise in the wide region of  $\dot{\gamma}$  it is not. The power law rheological model

$$\eta_a = \frac{\tau}{\dot{\gamma}} = K \cdot \dot{\gamma}^{n-1} \quad (1)$$

was used to describe this relation. The power  $n$  represents the flow behavior index of the fluid (referred as:  $n = 1$  for a Newtonian fluid, less than 1 for a shear thinning fluid and greater than 1 for a dilatant fluid), while the coefficient  $K$  represents the index of fluid consistency. Both quantities were measured (with a HAAKE viscosity meter type Rotovisco RV 100 equipped with a thermostat) at the same temperature as in measurements in mixing of fluid and in dispersing of air into fluid, respectively.  $K$  and  $n$  were always measured soon after the experiments were finished. To detect the temperature dependency of  $K$  and  $n$ , a set of measurements was performed; the resulting data are given in Table 2. Comparing only the influence of temperature on apparent viscosity, the relative difference defined as  $(\eta_{\vartheta_{\min}} - \eta_{\vartheta_{\max}})/\eta_{\vartheta_{\min}}$  was found to be:

- in  $0.5 \%$  CMC; up to  $0.2 \%$  in mixing of liquid and between  $3.1 - 5.4 \%$  in aerating
- while in  $1 \%$  CMC the differences were between  $2.1 - 4.4 \%$  and  $2.1 - 2.5 \%$  in mixing and aerating, respectively.

A test was made to check the mechanical degradation of CMC solution in mixing over several hours. No significant differences were found in measured values of  $K$  and  $n$  before and after mixing. As can be found in the literature,<sup>14</sup> the viscosity of a  $w = 0.4 \%$  CMC solution was found to decrease by less than  $10 \%$  after six days of continuous shearing in the stirred vessel. For the power consumption measurements, the effect of degradation was negligible since the duration of separate measurement was less than two hours.

The degassing of viscous fluids, especially non-Newtonian fluids, is a difficult task from an experimental point of view. In a mixing tank, as is well known, the apparent viscosity decreases from its maximum value near the vessel wall (lowest shear rate) to the vicinity of the stirrer where the shear rates are greatest. Complex fluids present a generally viscoelastic character, especially when

stirring is stopped or even at low shear conditions, which induces an apparent decrease in the viscosity of the CMC solution after aeration. This phenomenon can be explained by the fact that tiny bubbles remained captured in the fluid, which influenced the rheological properties. In some fermentation processes when broth rheology changes rapidly with fermentation time, samples of broth have been taken periodically to characterize the biomass. These test samples also contain dispersed fine bubbles, which probably influence the rheological properties similarly.<sup>18–22</sup> As shown in Fig. 2, the apparent viscosity of the 1 % CMC solution after aeration showed, quite coincidentally, very close values at all shear stresses to the 0.5 % CMC solution before aeration. To avoid further temperature influence, only the values at the same temperature, i. e. 20.5 °C, were compared in Fig. 2. All other representative values for all sets of measurements are included in Table 2.

**Mixing power**

Mixing power was calculated based on measured torque and rotational impeller speed according to:

$$P = 2 \cdot \pi \cdot n_s \cdot M. \tag{2}$$

The value of maximum shear rates was estimated in the impeller region as well as in a bulk re-

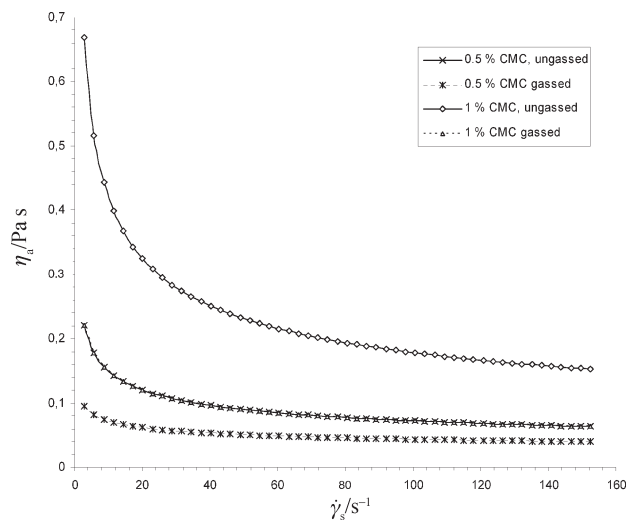


Fig. 2 – Apparent viscosity  $\eta_a$  vs. shear rate  $\dot{\gamma}$  in aqueous CMC solution at reference temperature  $\vartheta = 20.5 \text{ }^\circ\text{C}$

gion. On this basis, the Reynolds number can be obtained by the Metzner-Otto correlation. The average shear rate of CMC solutions was expressed for a shear thinning fluid:

$$\dot{\gamma} = k_s \cdot n_s \tag{3}$$

where  $k_s$  denotes a shear rate constant dependent only on stirrer type. According to literature data, the appropriate shear rate constant of a Rushton turbine can be found in the range from 10 to 11.6<sup>11,12,16</sup>,

Table 2 – Measured values of  $K$  and  $n$  in mixing and air-dispersion

Fluid	$\vartheta$ [°C]	Without aeration		After aeration	
		$n$	$K/\text{Pa s}^{-n}$	$n$	$K/\text{Pa s}^{-n}$
0.5 % CMC	20	0.669	0.344	0.781	0.119
	20.5	0.684	0.309	0.845	0.082
	21.4	0.693	0.304	/	/
	21.5	/	/	0.832	0.084
	22	/	/	0.831	0.083
	22.5	/	/	0.807	0.096
	22.7	0.685	0.301	/	/
	22.9	/	/	0,775	0,116
1.0 % CMC	20	/	/	/	/
	20.5	0.628	0.99	/	/
	21	0.623	1.001	0.669	0.343
	21.4	/	/	0.685	0.315
	21.5	0.634	0.94	/	/

where those adopted values were recommended for high-speed impellers. On the other hand, *Nouri* and *Hockey*<sup>14</sup> have recently found that a shearing constant of 54 provided better correlation between the power numbers of Newtonian fluids and CMC solutions. This value was taken as a validation of our experimental data. Finally, the apparent viscosity of the fluid in mixing with a Rushton turbine was re-calculated as:

$$\eta_a = K \cdot (54 \cdot n_s)^{n-1}. \quad (4)$$

Considering the eqs. (3) and (4) the Reynolds number can be written as:

$$Re = \frac{\rho \cdot n_s^{2-n} \cdot D^2}{K \cdot 54^{n-1}} \quad (5)$$

All the measurements, including both single- and two-phase mixing, respectively were taken in the range  $39 \leq Re \leq 7689$ . Due to temperature dependency of the viscosity, the fluid temperatures were measured as well; a detailed description can be found in reference.<sup>5</sup>

## Results and discussion

### Mixing power in single phase

Mixing of the CMC-water solution was performed in the range  $39 \leq Re \leq 2914$  in 1 % CMC and  $105 \leq Re \leq 6556$  in 0.5 % CMC, respectively. The dependence of power vs. Reynolds number is depicted in Fig. 4 with full lines marked as ungasged. As may be seen in both CMC solutions, a significant steep increase of the Power number, indicating a transition to laminar regime, occurred with decreasing the Reynolds number (impeller speed) from its minimum at  $Re \approx 362$  and  $Re \approx 880$  for 1 % and 0.5 % CMC solution, respectively. Further increasing of impeller speed led to a slight rise of the Power number values in both solutions. The results were consistent with the fact that increasing impeller speed led to decreasing the apparent viscosity, which controlled the impeller discharge flow. At  $Re \geq 1640$  the curves overlapped. From this value, a further increase of impeller speed gave identical values of  $Po$ , which can be indicated as the beginning of induced turbulence that prevailed over the viscosity. In the region  $Re \geq 1640$ , the average value of both solutions was found to be  $Po = 4.52$ , otherwise the power numbers increased slightly with Reynolds number and are in good agreement with measured data of *Nouri* and *Hockey*.<sup>14</sup> On the other hand, a plateau value of  $Po = 5.13$  was measured<sup>1</sup> for a Newtonian fluid in the region  $Re \geq 2.5 \cdot 10^4$  by using the same setup where tap water was used as a working fluid.

### Mixing power in air-dispersion

Actually, the Power number depended on gas-filled cavity structures, which affected the impeller pumping efficiency. The bigger the cavities, the weaker the radial discharge two-phase flow, which was detected by visual observation through the vessel wall. These phenomena were dependent on the rheological properties of the fluid as can be found from the literature.<sup>7,13,15</sup> For an exact understanding of mixing power drawn, it is necessary to know the ‘rules’ of gas-filled cavity structures. Recently,<sup>3</sup> gas-filled cavity structures in air-dispersion in shear thinning fluid were analyzed using the same experimental setup. It was found that gas-filled cavities in CMC solutions became more distinctive than those in water. First, they were larger, with a slightly different shape. Moreover, another phenomenon was found, i.e. large gas-filled cavities remained behind the impeller blades after the air was cut off, similarly as found in highly viscous Newtonian fluids.<sup>15</sup> Full details of the experimental work outlined here and the criterion for gas-filled cavity structure recognition has been described in detail.<sup>2</sup> Gas-filled cavity structures in the dispersion of air into aqueous CMC solutions can be divided into: (i) stable structures with cavities persistent at the same blades throughout the dispersion, i. e. vortex-clinging structure (*VC*), structure with two large cavities (*2L*), structure with three bigger and three smaller large cavities (*33*), structure with six equal-sized large cavities (*L6*) and ragged cavity structure (*R*), respectively; and (ii) transitional structures with sporadic appearance of one, two or three bigger cavities, i. e. structures with one (*1L*), (*1L-33*) or two (*1L-2L*), (*2L-33*) bigger cavities, respectively.

The corresponding flow regime map is depicted in Fig. 3 with experimental data marks shown for both aqueous CMC solutions. To find out the dependency of gassing power on  $Re$  and  $Fl$  numbers, aeration was done at three constant gas flow rates:  $Q = 1.55, 2.5$  and  $5 \text{ m}^3 \text{ h}^{-1}$  (corresponding superficial velocities  $v_s = 2.71 \cdot 10^{-3}, 4.37 \cdot 10^{-3}$  and  $8.73 \cdot 10^{-3} \text{ m s}^{-1}$ , respectively) and increasing rotational impeller speed stepwise while frequency was kept constant during the measurement. As may be seen from Fig. 3, the majority of data at  $Fr > 0.043$  corresponded to the stable 33 structure with a trend to *complete dispersion* regime at higher  $Fr$  numbers, and conversely, at low  $Fr$  the flooding regime and even a *bubble column* regime was found, respectively.

The effect of aerating at different gas flow rates into CMC solutions may be given as the relation power vs. Reynolds number as depicted in Fig. 4 (dashed lines). The resulting measured gassing  $Po$



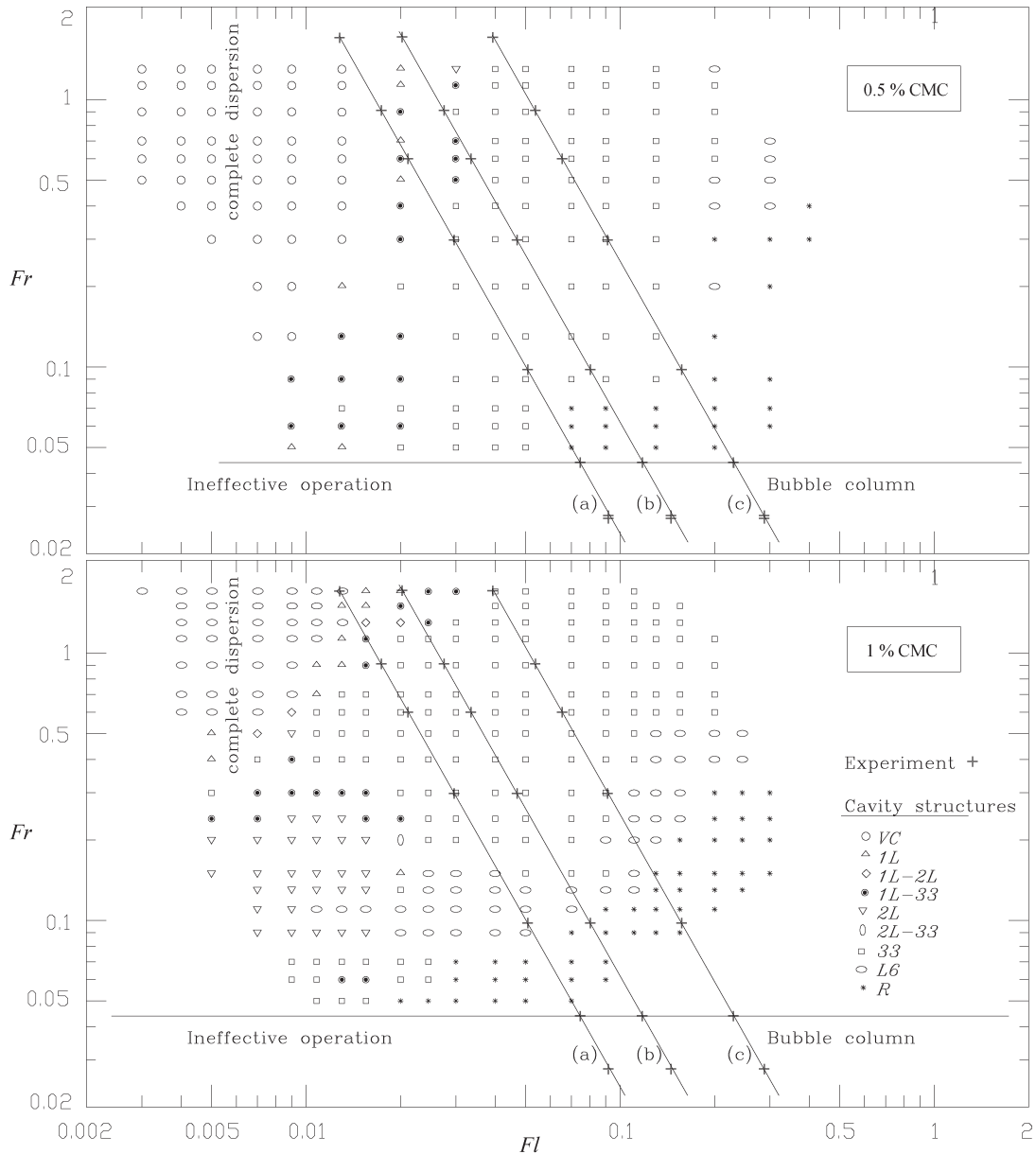


Fig. 3 – Flow regime map in aqueous CMC solution with marked sets of experimental data at different gas flow rates: (a) 1.55, (b) 2.5 and (c) 5 m<sup>3</sup> h<sup>-1</sup>, respectively

numbers were of lower values compared to ungasged, reaching the minimum at higher *Re* numbers. The increased apparent viscosity of 1 % CMC solution compared to 0.5 % CMC resulted as a ‘shift’ from higher to lower *Re* numbers, which may be observed in both operations of mixing and aerating, respectively. At high viscosities, i. e. low Reynolds numbers, no affect of aeration was observed; aerated results at three different gas rates were overlapping in 1 % CMC and two in 0.5 % CMC, respectively. The corresponding flow regimes were found as an ineffective operation and flooding represented by ragged cavity structure (*R*), see Fig. 3. Above a critical Reynolds number ( $Re_{w1\%} = 489$  and  $Re_{w0.5\%} = 720$ ) these curves separated from one another according to the value of the

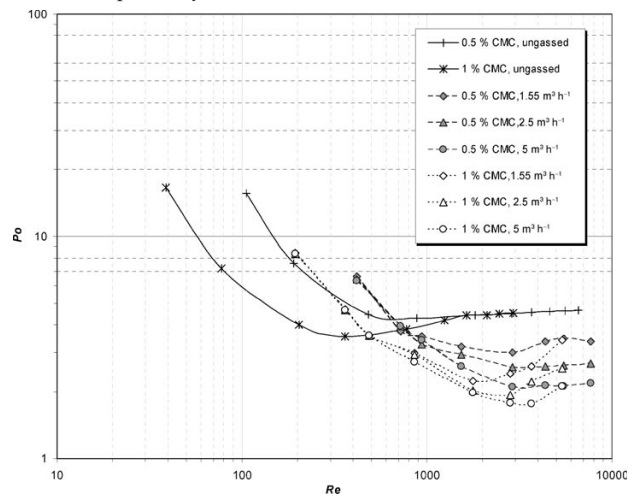


Fig. 4 – *Po* number vs. *Re* number by mixing and aerating into aqueous CMC solution

gassing rate: the higher the gassing rate the greater the power reduction, see Fig. 4. A similar value ( $Re_c = 500$ ,  $\eta = 0.2$  Pa s) was reported by Ozcan et al.<sup>15</sup> studying the effect of viscosity and power characteristics in a Newtonian fluid.

The minimum Power number values in 0.5 % CMC solution at all three gas rates were found at a Reynolds number of 2908, approximating to a rotational impeller speed of  $n_s = 266$  rpm (i. e.  $Fr = 0.3$ ). According to Fig. 3, at  $Fr = 0.3$  a stable 33 gas-filled cavity structure was found at the impeller blades. The results in the 1% CMC solution were similar, where three different minimum values of Power number were found corresponding to  $Fr = 0.9$ , 0.6 and 0.3 at gas flow rates of 5, 2.5 and  $1.55$  m<sup>3</sup> h<sup>-1</sup>, respectively. The minima of gassing  $Po$  number corresponded to stable 33 structures, while increasing rotational impeller speed expressed by Froude number led to better (complete) recirculation of liquid bulk in the vessel, as may be clearly seen in the flow regime map, see Fig. 3. Conversely, the decreasing of rotational impeller speed (i.e.  $Re$  number in Fig. 4,  $Fr$  number in Fig. 3, respectively) demonstrated a rising effect of viscosity, which caused the stirred vessel to operate under flooding regime or even as a bubble column, see Fig. 3.

The dependence between gassing power and aeration rate expressed by  $Fl$  number for different  $Re$  numbers is depicted in Fig. 5. The gassing power is not reduced by aeration below a Reynolds number of 856 where viscosity prevailed. This is consistent with our results concerning the gas-filled cavity structures: cavities remain attached behind the blades (1L). When this  $Re$  value was exceeded, the gassing power became dependent on the aeration rate. In a transitional as well as in a turbulent regime the gas-filled cavity structure controls the discharge two-phase flow and consequently the bulk circulation; the higher the gassing rate the lower the circulation.

The experimental results shown in Fig. 6 depict the relation of  $P_g/P$  vs.  $Fl$  number. At the beginning of aeration,  $P_g/P$  decreased very steeply at lower airflow rates expressed with  $Fl$  number, and after that the decrease became much slighter with further increasing of the airflow. This was evident from all curves and in both CMC-water solutions. In aeration in a CMC solution, the power drop at  $Fr$  equal to 0.3, 0.6 and 0.9 was higher than that at  $Fr = 0.1$  which seemed to be almost independent of the airflow rate. Especially in the case of 1 % CMC, where the effect of the viscosity prevailed over the dissipating power of the impeller discharge flow, as was seen from visual observations, huge cavities formed behind the blades, which ceased the radial discharge flow. The stirred vessel operated under

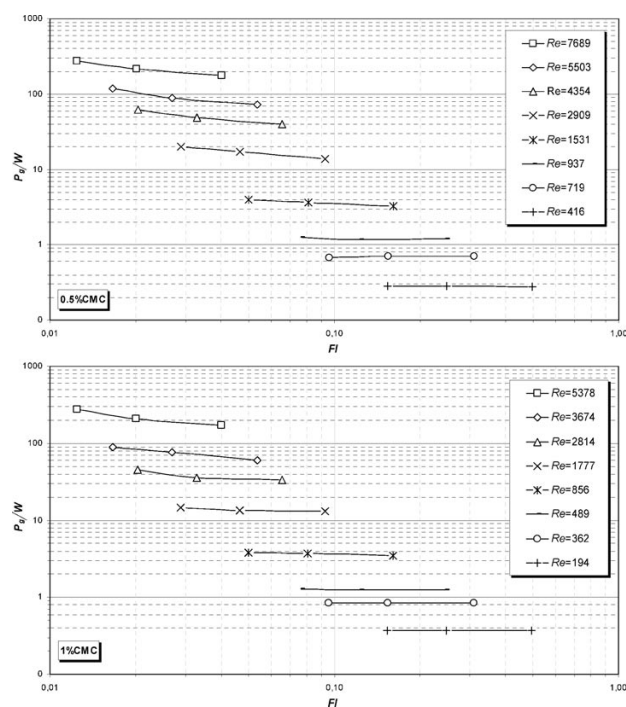


Fig. 5 – Gassing power vs.  $Fl$  number by air-dispersion in 1 % CMC-water solution at different  $Re$  numbers

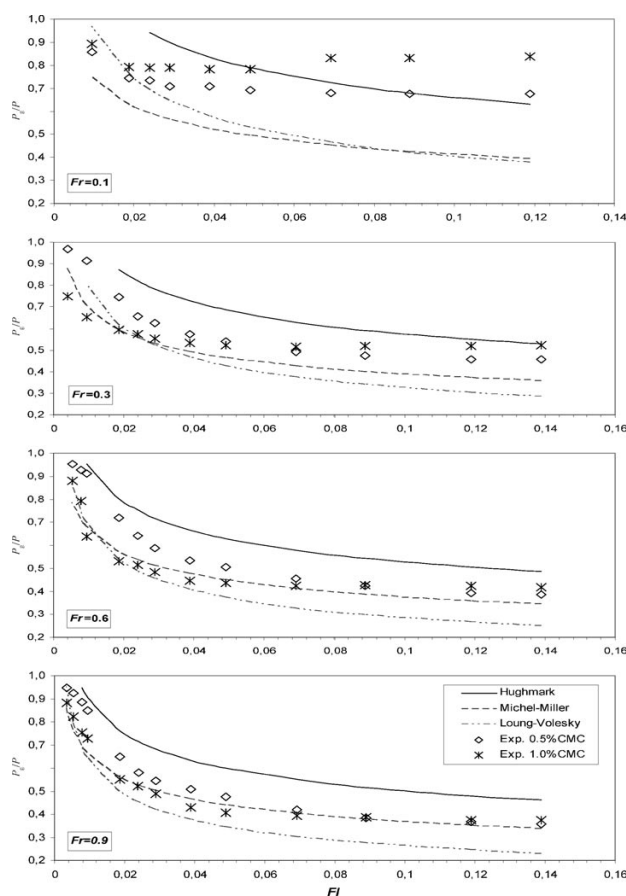


Fig. 6 – Comparison between experimental data and correlated data from literature

the flooding condition, recognized by two independent parameters: typical increasing of  $P_g/P$  ratio when flooded and from gas-filled cavity structures ( $R$ ) in Fig. 3 for corresponding regimes.

### Comparison of results with correlations in literature

The measured values of  $P_g/P$  ratio in air-dispersion in CMC solution were compared to those obtained from correlations found in literature for the same fluids. Michel and Miller<sup>10</sup> reported aerated power data with several fluids in vessels of different diameter. The given correlation was:

$$P_g = 0.706 \cdot \left( \frac{P^2 \cdot n_s \cdot D^3}{Q^{0.56}} \right)^{0.45} \quad (6)$$

Loung and Volesky<sup>9</sup> correlated the data from a relatively small vessel for a non-Newtonian liquid separately in the form:

$$\frac{P_g}{P} = 0.514 \cdot \left( \frac{\rho \cdot n_s^2 \cdot D^3}{\sigma} \right)^{-0.194} \cdot \left( \frac{Q}{n_s \cdot D^3} \right)^{-0.38} \quad (7)$$

Hughmark<sup>8</sup>, capturing data of other researchers who carried out experiments at different vessel dimensions,  $D/T$  ratio and fluids, published the following correlation:

$$\frac{P_g}{P} = 0.1 \cdot \left( \frac{n_s^2 \cdot D^4}{g \cdot w_b \cdot V^{0.667}} \right)^{-0.2} \cdot \left( \frac{Q}{n_s \cdot V} \right)^{-0.25} \quad (8)$$

Detailed geometrical and other conditions of the above correlations are given in Table 3.

A comparison between measured and correlated results as the relation of  $P_g/P$  vs.  $Fl$  number in aerating in 0.5 and 1.0 % aqueous CMC solutions is given in Fig. 6. At low impeller speed (i.e.  $Fr =$

0.1), and at both fractions no correspondence between measured and correlated data can be found; the nearest were Hughmark's approximated data. With increasing impeller speed ( $Fr$ ) the correspondence improved, especially with the Michel-Miller correlation at both concentrations as may be seen in Fig. 6 at  $Fr = 0.6$  and  $0.9$ , respectively. Surprisingly, while the Hughmark correlation based on groups of datasets of different vessel scale and fluids originally has an absolute deviation of 8.5 %, here it did not fit well. In general, the highest values of  $P_g/P$  were correlated by the Hughmark, while the lowest was given by the Loung-Volesky correlation. In spite of forming a separate correlation for non-Newtonian fluids, in the latter case the wall effects due to small vessel dimensions could be the reason for disagreement with our data.

According to the literature, the above-mentioned correlations described power decrease well in a Newtonian fluid; otherwise in a shear thinning fluid the correspondence was satisfactory. The correlations applying to non-Newtonian fluids should include apparent viscosity.

### Conclusions

All experiments were performed in a pilot-scale mixing vessel using a shear thinning model fluid of CMC-water solutions at  $w = 0.5$  and  $1$  %.

When mixing in a single phase a significant steep increase of the Power number occurred with decreasing of the Reynolds number, indicating a transition to laminar regime. Increasing of the Reynolds number led to a slight increment of the Power number value once the minima were reached (in a transitional regime) at  $Re \approx 362$  and  $Re \approx 880$  for  $w = 1$  % and  $0.5$  % CMC solution, respectively. The condition at  $Re \approx 1640$  found in the power vs. Reynolds

Table 3 – Geometrical and other conditions for given correlations

Correlation Property	Michel – Miller	Hughmark	Loung – Volesky	Present experiment
$T$ , m	0.165 – 0.29	0.165, 0.222, 0.25, 0.29, 0.305, 0.457, 0.48, 1.0	0.222	0.45
$D/T$	0.25 – 0.47	0.23 – 0.5	0.333	0.333
$\rho$ , kg m <sup>-3</sup>	800 – 1650	800 – 1600	983 – 1104	1000, 1002
$\sigma$ , N m <sup>-1</sup>	0.027 – 0.072	0.025 – 0.073	0.055 – 0.072	0.071, 0.070
$\eta$ , Pa s	$0.9 \cdot 10^{-3} - 100 \cdot 10^{-3}$	$0.8 \cdot 10^{-3} - 90 \cdot 10^{-3}$	$0.85 \cdot 10^{-3} - 3 \cdot 10^{-3}$	0.065 – 0.516
$Q$ , m <sup>3</sup> s <sup>-1</sup>	$9.5 \cdot 10^{-6} - 4.7 \cdot 10^{-4}$	/	/	$1.028 \cdot 10^{-4} - 13.88 \cdot 10^{-4}$
$Fl$	0.0021 – 0.0850	/	0.005 – 0.060	0.012 – 0.140
$Fr$	/	/	0.7 – 1.55	0.1, 0.3, 0.6, 0.9

number relation with overlapped curves of different solutions may be indicated as the beginning of induced turbulence, which prevailed over the viscosity.

Actually, the Power number in air-dispersion depended on gas-filled cavity structures, which affected the impeller pumping efficiency. The structures were dependent on the rheological properties of the fluid; in shear thinning fluid, it was found that gas-filled cavities in CMC solutions became more distinctive than those in water. As may be observed from the flow regime map, the majority corresponded to the stable 33 structure with a trend to *complete dispersion* regime at higher impeller speeds, and conversely, the *flooding* regime and even a *bubble column* regime was found, respectively, at lower speeds. In general, the highest power drop was found with the largest amount of introduced air with an exception at low impeller speed in 1 % CMC solution, where viscosity prevailed over induced turbulence.

A comparison between measured and correlated  $P_g/P$  values from literature was given. Surprisingly, the best correspondence was found only for higher  $Fr$  numbers with the Michel Miller correlation, while the Hughmark correlation based on groups of datasets of different vessel scale and fluids did not fit well here. The correlations applying to non-Newtonian fluids should include apparent viscosity.

#### ACKNOWLEDGMENT

The authors wish to thank the Slovenian Ministry of Science for financial support under the current Project No. J2-7517.

#### Nomenclature

$g$	– gravity, $\text{m s}^{-2}$
$D$	– impeller diameter, m
$K$	– the fluid consistency index, $\text{Pa} \cdot \text{s}^{-n}$
$k_s$	– shear rate constant
$M$	– mixing torque, N m
$n_s$	– impeller speed, $\text{s}^{-1}$
$n$	– the flow behavior index of the fluid
$P$	– mixing power, W
$Q$	– volumetric gas flow rate, $\text{m}^3 \text{s}^{-1}$
$T$	– tank diameter, m
$V$	– liquid volume, $\text{m}^3$
$v_s$	– superficial velocities, $\text{m s}^{-1}$
$w_b$	– blade width, m
$Fl$	– Flow number, $Q/(n_s \cdot D^3)$
$Fr$	– Froude number, $D \cdot n_s^2 / G$
$Po$	– Power number, $P/(\rho \cdot n_s^3 \cdot D^5)$
$Re$	– Reynolds number, $n_s \cdot \rho \cdot D^2 / \eta$
$w$	– mass fraction, %

#### Greek symbols

$\rho$	– density, $\text{kg m}^{-3}$
$\eta$	– viscosity, $\text{Pa} \cdot \text{s}$
$\nu$	– kinematical viscosity, $\text{m}^2 \text{s}^{-1}$
$\sigma$	– surface tension, $\text{N m}^{-1}$
$\tau$	– shear stress, Pa
$\dot{\gamma}$	– shear rate, $\text{s}^{-1}$
$\vartheta$	– temperature, $^{\circ}\text{C}$

#### References

- Bombač, A., J. Mech. E. **44** (1998) 105.
- Bombač, A., Žun, I., Filipič, B., Žumer, M., AIChE J. **43** (1997) 2921.
- Bombač, A., Žun, I., Žumer, M., Turk, J., Gas filled cavity structure in a pseudo plastic fluid agitated by Rushton turbine, in Štok, B. (Ed.), Kuhljevi dnevi '96, Slovensko društvo za mehaniko, Ljubljana, 1996, pp 193–200.
- Bombač, A., Žun, I., Gas-filled cavity structures and local void fraction distribution in vessel with dual-impellers, in Van den Akker, Derksen (Eds.), Mixing X, Elsevier Science B.V., Amsterdam, 2000, pp 469–476.
- Dževerdanovič, Z., Poraba energije pri mešanju in dispergiranju zraka v psevdoplastično tekočino, Diploma thesis, FKKT, Ljubljana, 1996.
- Espinosa-Solares, T., Brito-De la Fuente, E., Tecante, A., Tanguy, P. A., Chem. Eng. Technol. **25** (2002) 723.
- Middleton, J. C., Gas-liquid dispersion and mixing, in Harnby N., Edwards M. F., Nienow A. W. (Eds.), Mixing in the Process Industries, Butterworth-Heinemann, Oxford, 1992, pp 322–362.
- Hughmark A. G., Ind. Eng. Chem. Process Des. Dev. **19** (1980) 638.
- Luong H. T., Volesky B., AIChE.E.J. **25** (1979) 893.
- Michele B. J., Miller, S. A., AIChE.E.J. **8** (1962) 262.
- Mishra, V. P., Kumar, P., Joshi, J. B., Chem. Eng. J. **71** (1) NOV 1998, 11–21.
- Montante, G., Moštěk, M., Jahoda, M., Magelli, F., Chem. Eng. Sci. **60** (2005) 2427.
- Nienow A. W., Wisdom D. J., Solomon J., Machon W., Vlceh J., Chem. Eng. Commun. **19** (1983) 273.
- Nouri, J. M., Hockey, R. M., J. Chem. Eng. Jpn. **31** (1998) 848.
- Ozcan, N. G., Decloux, M., Bruxelmane, M., Chem. Eng. Res. Des. **68** (1990) 63.
- Vlaev, S. D., Valeva, M. D., Mann, R., Chem. Eng. J. **87** (2002) 21.
- Žun, I., Bombač, A., An Application of Local Void Fraction Measurements in Discharge Flow of Single and Dual Rushton Impellers, in Bertrand, J., Villermaux, J. (Eds.), Mixing IX – Multiphase Systems, Vol. 11, Technique et Documentation-Lavoisier, Paris, 1997, pp. 153–0.
- Lopez, J. L. C., Perez J. A. S., Sevilla J. M. F., Porcel, E. M. R., Chisti, Y., J. Biotechnol. **116** (2005) 61.
- Lopez, E., Ramos, I., Sanroman, M. A., Journal of Food Engineering **60** (2003) 463.
- Brar, S. K., Verma, M., Tyagi, R. D., Valero, J. R., Surampalli, R. Y., Water Research **39** (2005) 3001.
- Zhang, W., Li Z. J., Agblevor, F. A., Process Biochemistry **40** (2005) 2073.
- Koutinas, A. A., Wang, R., Kookos, I. K., Webb, C., Biochemical Engineering Journal **16** (2003) 23.